Structural and electronic properties of the quasi-one-dimensional metallic chains of the Au-induced facets on the Si(5 5 12) surface

S. S. Lee, N. D. Kim, C. G. Hwang, H. J. Song, and J. W. Chung*

Physics Department and Basic Science Research Institute, Pohang University of Science and Technology, San 31 Hyoja Dong, Pohang 790-784, Korea

We have investigated the atomic arrangements and electronic properties of the quasi-one-dimensional (Q1D) atomic chains of the Au-induced facets formed on the clean Si(5 5 12)-2×1 surface. The interchain distances of the two well ordered facet structures are estimated to be 30.2 and 22.8 Å. By utilizing linearly polarized synchrotron photons, we also determine a complete band diagram of the surface bands and their symmetry characteristics along the two high symmetry azimuths ($\bar{\Gamma} - \bar{M}$ and $\bar{\Gamma} - \bar{X}$) of the surface Brillouin zone. The Q1D nature of the Au-induced atomic chains has been well demonstrated by the extremely anisotropic band dispersions of the Au-induced surface bands in addition to the 2×1 surface morphology. We find that while the clean reconstructed Si(5 5 12)-2×1 surface is insulating, the Au-induced chains form a highly anisotropic metallic system.

PACS number(s): 73.20.−r, 73.50.−h, 68.43.−h

I. INTRODUCTION

With the advent of nanotechnology, much interest has been devoted to the fabrication of nanosized structures on solid surfaces. One of the potential applications of such nanostructures is to utilize their unique properties to develop more advanced devices such as a single-electron transistor, a quantum dot laser, and a quantum computer. Although a number of sophisticated experimental techniques using various forms of lithography[1] have been developed, adsorption on a highly stepped single crystalline surface has been used most extensively to form various nanosized structures on solid surfaces. Such stepped vicinal surfaces provide well defined binding sites for foreign adsorbates to grow various nanostructures such as quasi-zero-dimensional nanodots (or atom clusters), quasi-one-dimensional (Q1D) wires, and nanofilms through much efficient self-assembling processes.[2–7] The degree of steps, the kinds of substrate materials, and temperature (of both adsorbate and substrate) are major experimental variables to control with in order to produce a well defined nanostructure.

Despite the vast library for the structural studies of the Q1D nanostructures on vicinal silicon surfaces,[6–11] only a few have been made for the electrical properties of such Q1D nanostructures except the cases of the Au/Si(111) (Refs. 12–14) and Si(557)-Au (Refs. 15 and 16) systems. Such scarcity might be attributed partially to the difficulty in understanding the unusual behavior in photoemission data taken from Q1D nanowires, for example, the vanishing intensity at Fermi level even for a metallic wire and a complication due to the non-Fermi-liquid properties unique to the 1D nanostructures. Such an ambiguity has caused two contradictory interpretations on the temperature-induced band splitting for the Si(557)-Au surface as the lifting of degenerated surface bands at Fermi energy[16] and as the indication of the spin-charge separation[15] predicted by Luttinger and others for 1D metals rather than a typical Peierls transition.[17]

Here we provide photoemission data taken from Au-induced facet structures self-assembled on the Si(5 5 12) surface. Our data unambiguously show that the Au-induced Q1D chains are metallic along the direction parallel to the chains. This is seen by a unique dispersing surface band which crosses the Fermi level along the chain direction with a significant intensity. The surface band, however, remains dispersionless, with a binding energy fixed at about 1.0 eV below the Fermi level along the direction perpendicular to the chain direction. These Au-induced Q1D structures thus reveal a unique anisotropic band dispersions to exhibit a Q1D metallic nature.

The Si(5 5 12) surface is an energetically stable high-index surface 30.5° miscut from the [001] to the [111] orientations, as sketched in Fig. 1.[18] In contrast the Si(557) surface is a 9.5° miscut Si(111) surface toward the [11$\bar{2}$] direction. When this bulk-terminated Si(5 5 12) surface is
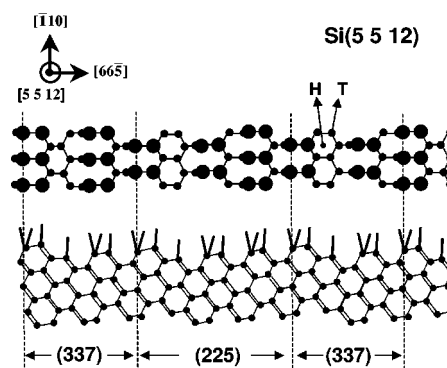
FIG. 1. Schematic drawings of the top view (upper panel) and the side view (lower panel) of the bulk-terminated Si(5 5 12) surface. The crystalline orientations [66$\bar{5}$], [$\bar{1}$10], and [5 5 12] referenced to the top view are indicated by the arrows above the top view. H and T indicate a hollow site and an on-top binding site for Au atoms. Note that the unit vector along the [66$\bar{5}$] direction consists of two unit vectors of the (337) surface and a single unit vector of the (225) surface. The short bars attached on the topmost Si atoms in the side view denote dangling bonds.

reconstructed to reduce its surface free energy, the periodicity along the $[\bar{1}10]$ direction becomes doubled with a unit cell of size 7.7×53.5 Å^2. Although the precise atomic arrangement of the reconstructed Si(5 5 12) surface is still under dispute, one finds that the long side of the unit cell along the $[\bar{6}65]$ direction, perpendicular to the long Si chains in the $[\bar{1}10]$ direction, consists of two unit cells of the (337) surface plus one unit cell of the (225) surface.[18−22]

II. EXPERIMENTAL DETAILS

We have utilized a combination of several surface diagnostic tools to investigate both the clean Si(5 5 12)-2×1 and the Au-induced facet structures on the Si(5 5 12) surface. A conventional rear view low-energy-electron diffraction (LEED) system has been used to probe changes in the atomic arrangement of the Au-induced facet structures on the Si(5 5 12) surface as a function of Au coverage. We have measured surface band structures using angle-resolved photoemission spectroscopy (ARPES) with linearly polarized synchrotron photons at the 3B1 beamline of the Pohang Light Source in Korea. The normal incidence monochromator beamline and its ARPES chamber provide overall energy and angular resolutions of ~ 100 meV and $\pm 1°$, respectively in the photon energy range from 13 to 29 eV. The base pressure of the ARPES chamber has been maintained below 1×10^{-10} Torr during the entire course of our measurements.

A Si(5 5 12) surface was prepared by cutting a Si(5 5 12) wafer purchased from Virginia Semiconductor INC into a ribbon shape with area of 18×5 mm^2. It is a phosphorus-doped Si(5 5 12) wafer with a resistivity of $\sim 2\Omega$ cm. The sample surface was heated resistively and its temperature was monitored by using an optical pyrometer. The sample surface was cleaned by repeatedly flashing at $1100°$C for 10 secs and then annealing at $700°$C for 5 min. The sample thus prepared showed a well-defined 2×1 LEED pattern with dark background indicating the clean reconstructed Si(5 5 12)-2×1 surface. We have confirmed the cleanness of the surface from the absence of any detectable signals of O $1s$ or C $1s$ peaks in our x-ray photoemission spectroscopy (XPS) data. A Au rod ($\phi \sim 1.6$ mm) wrapped with a tungsten filament ($\phi \sim 0.025$ mm) was used as a Au source. The deposition of Au was made by resistively heating the Au rod located about 5 cm ahead of the sample surface. The vacuum of the chamber has been maintained below 3×10^{-10} Torr during evaporation of Au while the sample was kept at $600°$C. We continually increased Au coverage until we observed a well-developed LEED pattern at room temperature. We then measured the Au core-level XPS peak to estimate the Au coverage. The Au-induced facet structures turned out to be remarkably inert, producing an almost identical valence band or Au core level even after extended hours. We have measured a set of ARPES spectra along the two major symmetry axes ($\bar{\Gamma}-\bar{M}$ and $\bar{\Gamma}-\bar{X}$) of the 1×1 surface Brillouin zone (SBZ) of the clean reconstructed Si(5 5 12)-2×1 surface. The linear polarization of synchrotron photons has been utilized to identify symmetry of the characteristic surface electronic states. The Fermi level (E_F) was determined by using a Ta clip attached to the Si sample.
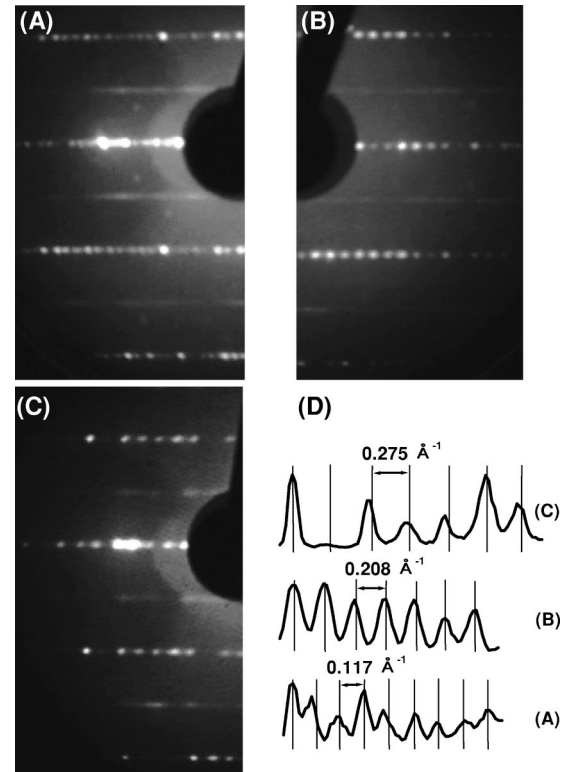
FIG. 2. LEED patterns observed from the clean reconstructed Si(5 5 12)-2×1 surface (A), the Au-induced (337)×2 facets (B), and the Au-induced (225) facets (C) depending on Au content. The doubled periodicity of the reconstructed 2×1 surface in (A) is indicated by the weak stripes between the lines of normal spots from the unreconstructed Si(5 5 12)-1×1 structure. (D) Intensity profiles of LEED spots along the $[\bar{6}65]$ direction for these surfaces. The interchain distance of the Au chains which is inversely proportional to the separation between two neighboring LEED spots in (B) and (C) can be determined when compared by the well known value of 53.5 Å from the separation in (A). The LEED beam energy was 88 eV.

III. RESULTS AND DISCUSSION

A. Interchain distances of the Au-induced facet structures

Figure 2(A) shows a 2×1 LEED pattern obtained from the clean reconstructed Si(5 5 12) surface at room temperature. The weak streaks between the lines of well defined diffraction spots along the $\bar{\Gamma}-\bar{M}$ direction indicate the doubled periodicity of the reconstructed surface from its bulk terminated 1×1 structure schematically drawn in Fig. 1. The atomic arrangement of the 2×1 reconstructed surface has been discussed intensively in terms of a combination of several structural elements such as dimers, tetramers, adatoms, and π-bonded chains (for example, see Fig. 5 in Ref. 18).[18−21] However, here we focus on the Au-induced changes of surface morphology. As shown in Figs. 2(B) and 2(C), we first observe two well-ordered Au-induced structures revealing essentially the same type 2×1 pattern. Previous scanning tunneling microscopy (STM) and reflection electron microscopy (REM) studies identified these ordered structures as particular types of the Au-induced Q1D chain-like facets,
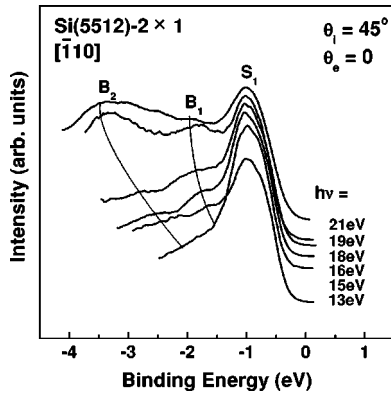
FIG. 3. Resonance photoemission spectra obtained from the clean reconstructed Si(5 5 12)-2×1 surface at normal emission geometry for photon energies ranging from 13 to 21 eV. The incident angle of the photon beam was kept fixed at $\theta_i = 45°$ with respect to the surface normal. Note that while the bulk bands B_1 and B_2 exhibit significant changes in binding energy with photon energy, the surface state S_1 remains fixed.

more specifically the $(337) \times 2$ facets [Fig. 2(B)] at 0.14 ML and the (225) facet [Fig. 2(C)] at 0.5 ML, respectively.[10,11]

The interchain distances of these facets determined by measuring the separation between the neighboring LEED spots [see the intensity profiles in Fig. 2(D)] are 30.2 and 22.8 Å, respectively. Note that these values are much shorter than the corresponding value of 53.5Å) of the clean 2×1 surface. Apparently the interchain distances decrease with increasing Au contents and turn out to be wider than that (19 Å) of the Au-induced Si(557) surface.[16] These values obtained are in excellent agreement with those for the facet structures observed by STM and REM. We thus identify the two ordered structures as the (337) and the (225) facets reported earlier.[10,11]

B. Electronic structure of the clean Si(5 5 12) surface

Figure 3 shows the energy distribution curves collected at normal emission geometry from the clean reconstructed 2×1 surface as a function of incident photon energy. The state S_1 at the binding energy of 1.1 eV, also observed earlier,[7,20] appears to be a surface state since its binding energy remains fixed with varying photon energy. Note that the two other states B_1 and B_2 change their binding energies significantly indicating that they are either surface resonances or bulk states.

The energy-momentum dispersions of the S_1 surface state are presented along the $[\bar{1}10]$ direction in Fig. 4(A) and the $[66\bar{5}]$ direction in Fig. 4(B). All the spectra were normalized by the incident photon flux. The Q1D nature of the S_1 band is well demonstrated by the extremely anisotropic dispersions along the two orthogonal directions, the $[66\bar{5}]$ and the $[\bar{1}10]$, which are perpendicular and parallel to the Si chains, respectively. Such an anisotropic feature, observed both in LEED and in the band dispersions, is quite consistent with previous observations.[7,18,20] Since the S_1 band does not cross the Fermi energy throughout the SBZ and the unit cell has an even number of dangling bonds, the surface has to be a Q1D
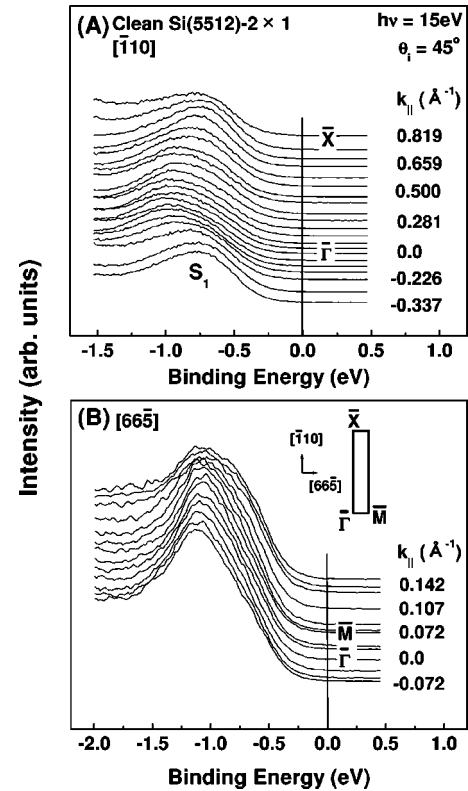
FIG. 4. Band dispersions of the surface band S_1 along the $[\bar{1}10]$ (or $\bar{\Gamma}$-$\bar{X}$) (A) and along the $[66\bar{5}]$ (or $\bar{\Gamma}$-$\bar{M}$)(B) of the clean reconstructed Si(5 5 12)-2×1 surface. Note the extremely anisotropic feature of the dispersions along the two perpendicular directions indicating a typical Q1D character of the state S_1. The inset in (B) shows the 1×1 SBZ.

band insulator in the scheme of a single electron band theory. The orbital nature of the S_1 is found to be primarily a p_z character probably from the buckled π-bonded chains of topmost Si adatoms,[23] as discussed below in Sec. III D.

C. Electronic structure of the Au-induced facets

We have also obtained changes in the valence band with photon energy (Fig. 5) and band dispersions (Fig. 6) of the characteristic surface bands of the two different Au-induced facet structures [the Si(337) and the Si(225)]. The two Au-induced states S_m and S_2, with binding energies of about 0.2 and 1.1 eV below the Fermi energy, are apparently surface states since their binding energies remain unaltered with varying photon energy, as seen in Fig. 5. Note that the remarkably enhanced intensities of these states at photon energy near 25 eV as also seen for other Au/Si systems.[13,16] Such a variation with photon energy at a fixed parallel component of electron momentum ($k_\parallel = 0.426$ Å^{-1}) mainly reflects the coupling to the final state wave function.[24] From the remarkably anisotropic band dispersions along the two azimuths $\bar{\Gamma}$-$\bar{X}$ and $\bar{\Gamma}$-$\bar{M}'$ (Fig. 6), one can clearly notice the Q1D nature of these surface states. Note the change of the zone boundary from $\bar{M}$ ($\pi/53.5 = 0.058$ Å^{-1}) of the clean reconstructed Si(5 5 12) surface to $\bar{M}'$ ($\pi/31.4 = 0.1$ Å^{-1})
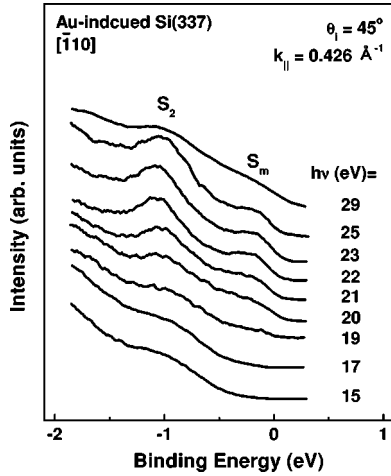
FIG. 5. Resonance photoemission spectra obtained from the Au-induced Si(337) facets at a fixed momentum ($k_\parallel = 0.426$ Å^{-1}) for photon energies ranging from 15 to 29 eV. Note that the two Au-induced surface states are most significant at photon energies in the range 20 eV $\leq \hbar\omega \leq$ 25 eV.

of the Si(337) facets. Interestingly enough the band dispersions of the two surface bands are almost identical for the (337) facets and the (225) facets.

The important observation to make from the dispersions is that the facets [both the (337) and (225)] are metallic only
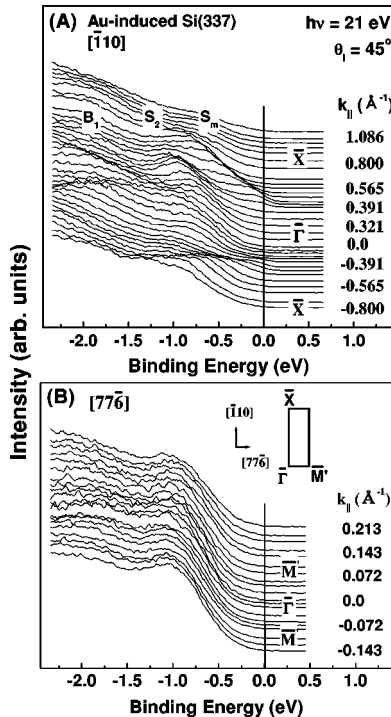
FIG. 6. Similar band dispersions of the Au-induced Si(337) facets as in Fig. 4 along the $\bar{\Gamma}$-$\bar{X}$ azimuth parallel to the Au-induced chain direction (A) and along the $\bar{\Gamma}$-$\bar{M}'$ azimuth perpendicular to it (B). Note that the surface state S_m clearly crosses Fermi level indicating metallic nature of the Au chains along the chain direction. The inset shows the 1×1 SBZ of the the Au-induced Si(337) facets.
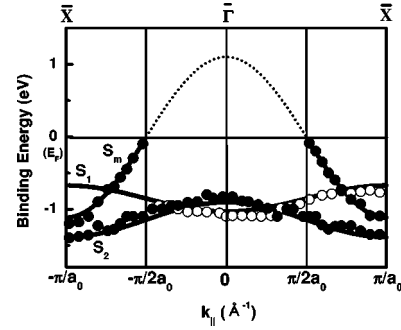
FIG. 7. Band diagram for the surface bands along the $\bar{\Gamma}$-$\bar{X}$ azimuth of the clean reconstructed Si(5 5 12)-2×1 surface (empty circles) and of the Au-induced Si(337) facets (filled circles). The solid curves and dotted curve drawn by extrapolating the data, are to guide the eye.

along the $\bar{\Gamma}$-$\bar{X}$ azimuth (parallel to the Au chains) while insulating perpendicular to it in a simple band picture. This is seen by the surface state S_m that clearly crosses the Fermi level along the $\bar{\Gamma}$-$\bar{X}$ azimuth but remains far from the Fermi level along the $\bar{\Gamma}$-$\bar{M}'$ azimuth. Such a feature is sharply contrasted to the insulating character of the clean Si(5 5 12)-2 ×1 surface (Fig. 4) but is quite similar to that of the Si(557)-Au surface.[15,16] As discussed later in Sec. III D, the state S_m has a p_z orbital character probably stemming from the Si dangling bonds of the facets. The origin of such a p_z orbital character of the Au-induced surface state is discussed further in Sec. III D. We summarized the dispersions as a band diagram in Fig. 7. From the dispersion of the S_m band that crosses the Fermi level at precisely one-half of the zone boundary, one may expect the Q1D metallic facets to exhibit a Peierls-like metal-insulator transition upon cooling below a certain transition temperature by forming a charge density wave with a doubled periodicity. An investigation to find such a Peierls-like transition is currently underway.

The metallic nature of these Au-induced facets may be understood qualitatively in terms of electron counting in a single electron band theory as discussed below. For the Si(337)-2×1 facets assuming the Au contents of about 0.1 ML,[10,11] we have an odd number (15) of electrons in each 2×1 unit cell [the 14 dangling bonds of the Si(337)×2 facets and one from each Au adsorbate], so that the facets may be metallic. Similar electron-counting also applies to the metallic Si(225) facets.

D. Orbital symmetries of the surface states of the clean Si(5 5 12)-2×1 and the Au-induced facets

We have measured the orbital symmetry of the surface states using linearly polarized synchrotron photons. According to the so-called Hermanson's rule,[24,25] one measures only the even component of a wave function with respect to a particular scattering plane when a detector is located within the scattering plane. A scattering plane here is defined by the propagation vector of incident photon beam and the outgoing momentum vector of photoelectron beam. This rule can easily be understood in terms of the Fermi golden rule, **I**
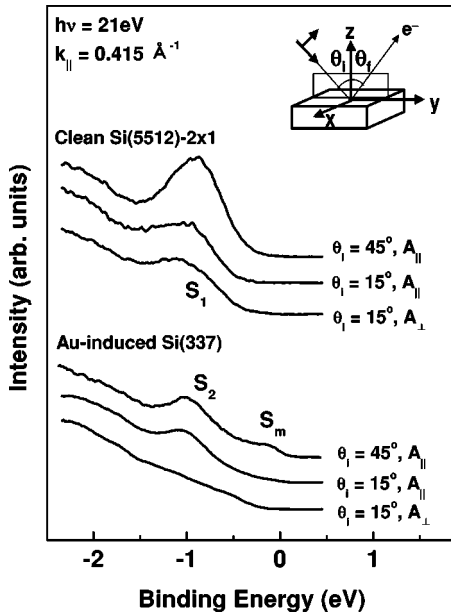
FIG. 8. Spectral changes as the scattering geometry changes by changing either the incidence angle θ_i of the photon beam or the outgoing angle θ_f of the photoelectrons to examine the symmetry of electron wave functions of the surface states. The photon energy was 21 eV and the momentum of photoelectron was kept fixed at $k_\parallel = 0.415$ Å^{-1} along the $\bar{\Gamma}$-$\bar{X}$ azimuth. Note that each surface state exhibits its unique behavior to show even orbital character with respect to the $(\bar{1}10)$ mirror plane. See the text for details.

$\sim 2\pi/\hbar \langle f|\mathbf{A} \cdot \mathbf{P}|i\rangle \delta(E_f - E_i - \hbar\omega)$, where **I**, **A**, and **P** are the intensity of a peak in photoemission spectrum, the vector potential of incident photon beam, and the momentum operator of a photoelectron, respectively. The states $|i\rangle$ and $|f\rangle$ denote initial and final states of the photoelectron excited by an incident photon of energy $\hbar\omega$. In order to detect an odd component, the detector should be located out of the scattering plane.

In order to determine the symmetry of a surface state with respect to a scattering plane, we utilized three different scattering geometries as sketched schematically in inset of Fig. 8: (1) $\theta_i = 45°$, detector-in, (2) $\theta_i = 15°$, detector-in, and (3) $\theta_i = 15°$, detector-out of the scattering plane. We conveniently took the $(\bar{1}10)$ symmetry plane as the scattering plane. We adopted photons of energy 21 eV which nearly maximizes the intensity of the surface states (see Figs. 3 and 5). The parallel component of electron momentum was fixed at $k_\parallel = 0.415$ Å^{-1} along the $\bar{\Gamma}$-$\bar{X}$ azimuth during our measurements. Apparently any z component should decrease upon changing the scattering geometry from (1) to (2), while an odd component should remain unaffected. Upon changing the scattering geometry from (2) to (3), however, any odd component should be enhanced while even component be unaltered.

For the surface state S_1 of the clean reconstructed 2×1 surface, the spectral behavior shown in Fig. 8 indicates an even character, probably of a p_z-type, as anticipated from the scattering geometry. The finite intensity for the geometry (3) is attributed to the z-component (even) of the wave function

excited by the remaining nonvanishing z component of the incident photon field. According to recent calculation, the π chains of the clean reconstructed Si(5 5 12) surface becomes significantly buckled to reach a minimum energy configuration.[26] The charge transfer accompanying the buckling then is likely to produce a dangling bonds of a p_z character as for the asymmetric dimers of the clean Si(100)-2 $\times$1 reconstruction.[27] For the Au-induced facets, the state S_m appears to behave almost the same way the S_1 of the clean surface does. This suggests that the S_m also has a p_z orbital character. The S_2 state, however, behaves quite differently from that of the S_1 or S_m, i.e., it stays almost unchanged in its intensity upon varying the scattering geometry from (1) to (2), while it disappears nearly completely at geometry (3). This indicates that the state S_2 has an in-plane even orbital character of $p_{x,y}$ type, so that the state remains unaffected when the z component of incident photon field varies. It is interesting to note that the two states S_1 and S_2, despite their nearly identical binding energies, exhibit quite different orbital symmetries.

Based on our observation presented in Fig. 8 and recent theoretical calculations, we conclude that S_1 has a p_z orbital character originating probably from the buckled Si π chains, and that S_2 has either a $p_{x,y}$ orbital character or an s-p hybridized orbital character stemming from the Au-Si bondings. It is somewhat surprising to find that the S_m has a p_z character also rather than an s-p hybridized orbital character as a Au-induced surface state. However, a small contribution from a Si-Au hybridized orbital, if any, to the S_m state may not be completely ruled out because of the weak but nonvanishing intensity barely observed at the scattering geometry (2). The fact that the S_m state has primarily a p_z orbital character suggests an important clue regarding to the binding sites for Au. If Au occupies an on-top site (see Fig. 1) of Si adatoms, it may waste some of the dangling bonds of Si adatoms by forming an s-p_z hybridization of which the character has not been found in Fig. 8. On the other hand, if Au occupies a hollow site, the Au-Si bonding would be an s-$p_{x,y}$ character rather than an s-p_z hybridization. We may then safely ascribe the S_2 state of a $p_{x,y}$ orbital character to the Au-Si hybridization. The confirmation of the binding sites of Au, however, demands a quantitative theoretical analysis of surface bands and their orbital characteristics which are not available at the present time.

IV. SUMMARY

We have observed two ordered Q1D Au-induced facets formed essentially by Au atoms introduced to the clean reconstructed Si(5 5 12)-2$\times$1 surface at an elevated temperature. We have confirmed the Q1D nature of the Au-induced chains both by observing well defined characteristic LEED patterns and by measuring the extremely anisotropic band dispersions of the Au-induced surface bands along the directions parallel and perpendicular to the chain direction. We find that these Au-induced atomic chains are metallic in a band picture only along the chain direction, and insulating perpendicular to it. In addition, we identify the symmetry properties of the surface states both of the clean recon-

structed Si(5 5 12)-2×1 surface and of the Au-induced Q1D facets by utilizing linearly polarized synchrotron photons. We find that the only surface state S_1 from the clean Si(5 5 12)-2×1 surface is of the p_z orbital character probably stemmed from the possible buckling of the π chains of the topmost Si atoms. We also find that the two surface states S_2 and S_m from the Au-induced facets are of $p_{x,y}$ (or s-p hybridized) character and of p_z character, respectively.

*Electronic address: jwc@postech. ac. kr; URL: http://www. postech. ac. kr/phys/snpl/

[1] See, for example, E. Kapon, D.M. Hwang, and R. Bhat, Phys. Rev. Lett. **63**, 430 (1989).

[2] S.P. Ahrenkiel, S.H. Xin, P.M. Reimer, J.J. Berry, H. Luo, S. Short, M. Bode, M. Al-Jassim, J.R. Buschert, and J.K. Furdyna, Phys. Rev. Lett. **75**, 1586 (1995); Phys. Today **49(5)**, 22 (1996).

[3] M.S. Miller, H. Weman, C.E. Pryor, M. Krishnamurthy, P.M. Petroff, H. Kroemer, and J.L. Merz, Phys. Rev. Lett. **68**, 3464 (1992); T. Jung, R. Schlittler, J.K. Gimzewski, and F.J. Himpsel, Appl. Phys. A: Solids Surf. **61**, 467 (1995).

[4] V. Bressler-Hill, A. Lorke, S. Varma, P.M. Petroff, K. Pond, and W.H. Weinberg, Phys. Rev. B **50**, 8479 (1994); C. Teichert, M.G. Lagally, L.J. Peticolas, J.C. Bean, and J. Tersoff, *ibid.* **53**, 16 334 (1996).

[5] F. Liu, J. Tersoff, and M. Lagally, Phys. Rev. Lett. **80**, 1268 (1998).

[6] A.A. Baski, K.M. Jones, and K.M. Saoud, Ultramicroscopy **86**, 23 (2001).

[7] S.R. Blankenship, H.H. Song, A.A. Baski, and J.A. Carlisle, J. Vac. Sci. Technol. A **17**, 1615 (1999); H.H. Song, K.M. Jones, and A.A. Baski, *ibid.* **17**, 1696 (1999).

[8] L. Seehofer, S. Huhs, G. Falkenberg, and R.L. Johnson, Surf. Sci. **329**, 157 (1995).

[9] M. Jałochowski and E. Bauer, Prog. Surf. Sci. **67**, 79 (2001).

[10] A.A. Baski, K.M. Saoud, and K.M. Jones, Appl. Surf. Sci. **182**, 216 (2001).

[11] Y. Peng, H. Minoda, Y. Tanishiro, and K. Yagi, Surf. Sci. **493**, 508 (2001).

[12] I.R. Collins, J.T. Moran, P.T. Andrews, R. Cosso, J.D. O'Mahony, J.F. McGilp, and G. Margaritondo, Surf. Sci. **325**, 45 (1995), and reference therein.

[13] R. Losio, K.N. Altman, and F.J. Himpsel, Phys. Rev. Lett. **85**, 808 (2000).

[14] H.W. Kim, K.S. Shin, J.R. Ahn, and J.W. Chung, J. Korean Phys. Soc. **35**, S534 (1999).

[15] P. Segovia, D. Purdie, M. Hensberger, and Y. Baer, Nature (London) **402**, 504 (1999).

[16] R. Losio, K.N. Altmann, A. Kirakosian, J.-L. Lin, D.Y. Petrovykh, and F.J. Himpsel, Phys. Rev. Lett. **86**, 4632 (2001).

[17] G. Grüner, *Density Waves in Solids*, 1st ed. (Addison-Wesley, Reading, MA, 1994).

[18] A.A. Baski, S.C. Erwin, and L.J. Whitman, Science **269**, 1556 (1995).

[19] S. Song, Mirang Yoon, and S.G.J. Mochrie, Surf. Sci. **334**, 153 (1995).

[20] W. Ranke and Y.R. Xing, Surf. Sci. **381**, 1 (1997).

[21] T. Suzuki, H. Minoda, Y. Tanishiro, and K. Yagi, Surf. Sci. **348**, 335 (1996); **357**, 522 (1996).

[22] Junliang Liu, Masaki Takeguchi, Miyoko Tanaka, Hidehiro Yasuda, and Kazuo Furuya, J. Electron Microsc. **50**, 541 (2001).

[23] See, for a review, Winfried Mönch, *Semiconductor Surface and Interface* (Springer-Verlag, New York, 1993), p. 155.

[24] S. D. Kevan, *Angle-Resolved Photoemission* (Elseivier, Reading, NY, 1992).

[25] E.W. Plummer and W. Eberhardt, Adv. Chem. Phys. **49**, 533 (1982).

[26] S. M. Jeong (unpublished).

[27] R.A. Wolkov, Phys. Rev. Lett. **68**, 2636 (1992).